Journal of Alloys and Compounds, 206 (1994) 263–266
JALCOM 1051

On new $CaBe_2Ge_2$-type representatives MAu_2Al_2

F. Hulliger, H.-U. Nissen and R. Wessicken
Laboratorium für Festkörperphysik ETH, CH-8093 Zürich (Switzerland)

(Received November 12, 1993)

Abstract

Rare-earth compounds with compositions near $LnAu_2Al_2$ (Ln = La · · · Nd, Sm · · · Dy) as well as $SrAu_2Al_2$, $ThAu_2Al_2$ and UAu_2Al_2 were found to crystallize in the tetragonal $CaBe_2Ge_2$ structure, tP10, space group P4/*nmm* (no. 129). Among these, only $EuAu_2Al_2$, $GdAu_2Al_2$, $TbAu_2Al_2$ and UAu_2Al_2 revealed (antiferro-)magnetic ordering above 2 K. No superconductivity was detected down to 1.8 K in $SrAu_2Al_2$, $LaAu_2Al_2$, $LaAu_{1.5}Al_{2.5}$ and $ThAu_2Al_2$.

1. Introduction

The series of the rare-earth elements (Ln) offers the possibility to study the influence of small changes in atomic size on various properties other than magnetic. Thus, the development of specific crystal structures in rare-earth series LnT_nX_m (T = transition element, X = B element) is a challenging crystal–chemical problem. We have recently made some efforts to contribute to the knowledge of the 1:2:1 compounds and reported on the preparation of new YPd_2Si-type representatives in the series $LnPd_2Ga$ [1] and $LnPd_2Al$ [2]. The orthorhombic YPd_2Si structure, an ordered version of the Fe_3C structure, is one of the three main types which occur among the ternary rare-earth intermetallics of composition LnT_2X, where T is a nickel-group transition element and X is one of the B elements Al, Ga, In or Si, Ge, Sn [3]. The predominant structure type is the cubic $CuMn_2Al$ (Heusler) type, an ordered derivative of the CsCl type, while the third type, the hexagonal $GdPt_2Sn$ type, an ordered version of the TiAs type, is much less frequent. The 1:2:1 rare-earth compounds with the coinage metals are known for X = In only, and they all crystallize in the Heusler type [3]. However, one Al compound with YPd_2Si structure, UAu_2Al, was reported by Takabatake *et al.* [4]. This compound orders antiferromagnetically below $T_N = 25$ K and has a fairly large electronic specific-heat term, $\gamma = 102$ mJ K^{-2} mol. From the existence of UAu_2Al we deduced a certain chance that the light rare-earth analogues would adopt the same structure. Our samples with Ce, Pr, Nd indeed gave similar X-ray patterns, though different from the expected ones. Moreover, the samples were not single-phase, even after annealing at 750 °C. Scanning electron microscope images of a specimen with bulk composition "$CeAu_2Al$" revealed at least three phases, one of which occurred as characteristic lath-shaped crystallites. Wavelength-dispersive X-ray microanalysis of these laths led to Ce:Au:Al concentrations of 20:41:39, 20.3:41.0:38.6, 21.0:43.2:35.8, 20.3:43.3:36.3, all in atomic per cent. Selected-area electron diffraction patterns finally established the presence of a phase with space group P4/*nmm*, which is compatible with the $CaBe_2Ge_2$-type structure.

2. Experimental details

Once the ideal composition of the new phase was known, an attempt was made to synthesize the whole series $LnAu_2Al_2$, starting with the lanthanum compound. Buttons weighing 1–2 g were obtained by reaction of the elements in an argon arc furnace. Annealing at 700 °C for two months did not significantly improve the quality of the samples. While the samples with La, Ce, Pr and Nd were fairly pure, those with the heavier Ln elements contained increasing amounts of foreign phases. The samples with Ln = Dy were very impure, and in the run with Ln = Ho no indication of a $CaBe_2Ge_2$-type phase was found, even after annealing several weeks at 800 and 650 °C.

Since the electron probe microanalysis of the $CaBe_2Ge_2$-type phase in the "$CeAu_2Al$" sample indicated an excess of gold, we conjectured the existence of a homogeneity region. It was therefore desirable to estimate the extent of this region from an analysis of the concentrations of the $CaBe_2Ge_2$-type phase in polyphase samples with compositions beyond the homogeneity limits. Therefore, samples with nominal compositions $CeAu_{2.5}Al_{1.5}$ and $CeAu_{1.5}Al_{2.5}$ were prepared.

SSDI 0925-8388(93)01051-5

The selected-area electron diffraction patterns, which led to the identification of the tetragonal phase, were made using a Philips CM 30 transmission electron microscope. Scanning electron micrographs were obtained on a JEOL JSM-840 instrument, using backscattered electrons in order to enhance the contrast between different phases. The microanalytical work was performed on a JEOL JXA-8800 (Sulzer Innotec) and a Cameca-SX 50 electron microprobe analyser (Institute for Crystallography, ETH).

The lattice parameters were derived from Guinier X-ray patterns taken with $CuK\alpha_1$ radiation and silicon (assuming $a = 5.43047$ Å at 295 K) as internal standard. The magnetic susceptibility was measured between 2 and 300 K, using a moving-sample magnetometer. For the superconductivity tests a magnetic field of 30–50 Oe was applied.

3. Results

The Guinier patterns of all compounds were indexed on the basis of the tetragonal $CaBe_2Ge_2$ structure, space group P4/*nmm* (no. 129). The structure type was confirmed by intensity calculations with the computer program LAZY PULVERIX [5] using the average site parameters $z_{Ln} \approx 0.249$, $z_{Au} \approx 0.63$ and $z_{Al} \approx 0.87$. The lattice parameters, listed in Table 1 and plotted in Fig. 1 as a function of the radii of the rare-earth ions, reveal a discontinuity of the *c*-axis data near the element samarium. Surprisingly, however, there is no such discontinuity of the *a*-axis data. This irregularity may possibly be explained by deviations in the stoichiometry. Indeed, electron-probe microanalyses of $GdAu_2Al_2$ yielded deviations from the ideal 1:2:2 stoichiometry, in contrast to $CeAu_2Al_2$ which turned out to be stoichiometric within the experimental errors. For the quenched sample the Gd:Au:Al proportion (as an average of five measurements) was 20.20:39.06:40.74, while for the annealed sample it was 20.23:38.23:41.54. This indicates a small shift towards higher Al concentrations, $LnAu_{2-\delta}Al_{2+\delta}$, $\delta \approx 0.1$, and appears to support our previous speculative assumption of a change in composition. (The Gd excess may rather indicate vacancies in the Au–Al sublattice, as are also present in the stannides $AnCo_{2-x}Sn_{2-y}$ and $AnNi_{2-x}Sn_{2-y}$, An = Th, U [6].) The lattice parameters of the off-stoichiometric Al-rich La and Ce compounds may be regarded as a further support of this explanation.

Both the Al-rich La and Ce samples $LnAu_{1.5}Al_{2.5}$ were found to be almost single-phase, still crystallizing in the $CaBe_2Ge_2$ structure, but with distinctly different lattice parameters. The composition $LnAu_{1.5}X_{2.5}$ is the composition at which the Ga analogues with Ln = La · · · Nd, Sm crystallize in the $CaBe_2Ge_2$ structure, whereas the compounds with higher gallium concentrations are disordered and adopt the $BaAl_4$ structure [7]. The electron microscope images of both $LaAu_{1.5}Al_{2.5}$ and $CeAu_{1.5}Al_{2.5}$ showed a striated pattern (Fig. 2), probably connected with concentration differences

TABLE 1. Room-temperature lattice parameters and X-ray densities of the $CaBe_2Ge_2$-type compounds (given as nominal compositions); space group *P4/nmm* (no. 129), tP10. The standard deviations added in parentheses refer to the statistical error only; the error due to calibration may be at least as large

Compound	*a* (Å)	*c* (Å)	*c/a*	*V* (Å^3)	d_X (g cm^{-3})
$LaAu_2Al_2$	4.4387(3)	10.3988(7)	2.3428(3)	204.88(4)	9.512
"$LaAu_{1.5}Al_{2.5}$"[a]	4.3844(4)	10.685(3)	2.437(1)	205.4(1)	8.11
"$CeAu_{2.5}Al_{1.5}$"[b]	4.4088(3)	10.3881(13)	2.3562(5)	201.92(6)	
$CeAu_2Al_2$	4.4077(3)	10.3917(13)	2.3576(5)	201.88(6)	9.673
"$CeAu_{1.5}Al_{2.5}$"[c]	4.3518(4)	10.672(2)	2.4523(7)	202.10(8)	8.25
$PrAu_2Al_2$	4.3892(4)	10.3895(10)	2.3670(4)	200.16(5)	9.770
$NdAu_2Al_2$	4.3727(3)	10.3915(10)	2.3764(4)	198.69(5)	9.897
"$NdAu_{1.92}Al_{1.92}$"	4.3572(6)	10.457(3)	2.400(1)	198.54(10)	
"$SmAu_2Al_2$"	4.326–4.337	10.45–10.515	2.41–2.43		
"$EuAu_2Al_2$"	4.4305(10)	10.487(5)	2.367(2)	205.9(2)	9.68
"$GdAu_2Al_2$"[d]	4.3005(5)	10.484(2)	2.438(2)	193.89(7)	10.37
"$TbAu_2Al_2$"	4.2828(4)	10.470(2)	2.445(1)	192.05(6)	10.49
"$DyAu_2Al_2$"	4.2675(8)	10.458(3)	2.451(2)	190.5(2)	10.64
$ThAu_2Al_2$	4.3003(8)	10.398(4)	2.418(2)	192.3(2)	11.74
UAu_2Al_2	4.2911(9)	10.424(3)	2.429(2)	191.9(2)	11.87
$SrAu_2Al_2$	4.4775(5)	10.482(3)	2.342(2)	210.2(2)	8.46

[a]Average $La_{0.9}Au_{1.55}Al_{2.45}$ according to microanalysis.
[b]Average $CeAu_2Al_{1.8}$ according to microanalysis.
[c]Average $CeAu_{1.4}Al_{2.3}$ according to microanalysis.
[d]Average $GdAu_{1.9}Al_{2.05}$ according to microanalysis.

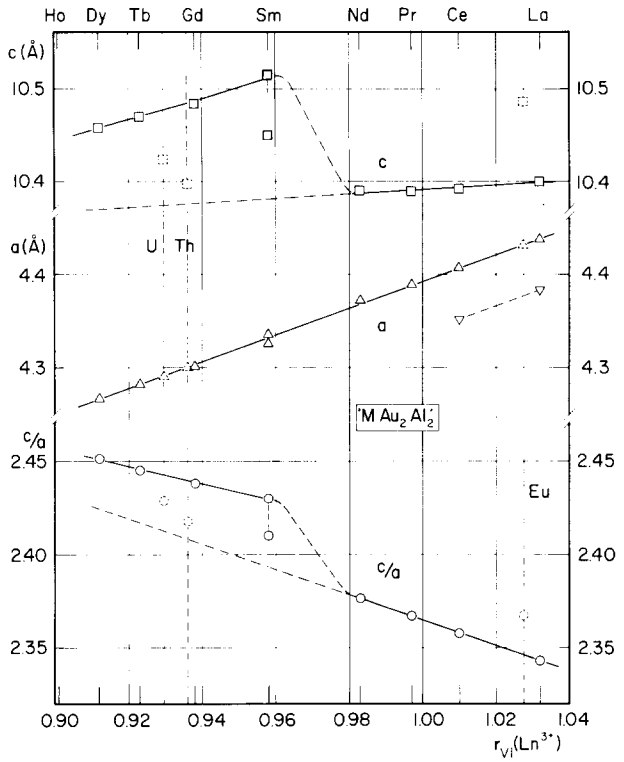

Fig. 1. Lattice parameters *a*, *c* and *c/a* of the $LnAu_2Al_2$ phases, plotted versus the Ln^{3+} radii after Shannon [8]. The broken symbols refer to the Th, U and Eu compounds adapted on the basis of the *a*-values. For $LaAu_{1.5}Al_{2.5}$ and $CeAu_{1.5}Al_{2.5}$ only the *a*-values are indicated; *c* and *c/a* are significantly higher than the values extrapolated from the Dy···Sm series.

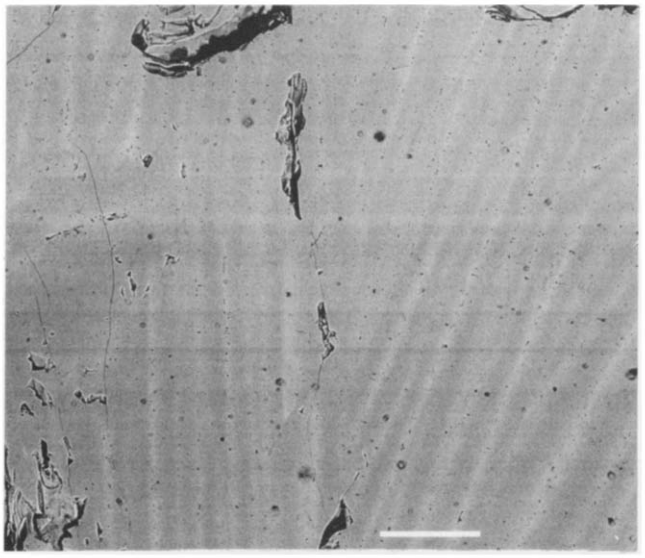

Fig. 2. Back-scattered electron microscope image of the Al-rich sample "$CeAu_{1.5}Al_{2.5}$". The darker areas are assumed here to be slightly richer in Al. Scale bar: 100 μm.

below the limit of resolution ("$LaAu_{1.5}Al_{2.5}$": Ln:Au:Al = 0.89:1.49:2.51 (d), 0.89:1.55:2.45 (g), twice 0.89:1.59:2.41 (g); "$CeAu_{1.5}Al_{2.5}$": 1:1.37:2.32 (d), 1:1.39:2.28 (g), 1:1.39:2.26 (d), 1:1.40:2.39 (d), where (d) and (g) refer to the dark and grey areas, respectively). In spite of the virtually identical images obtained of both the La and the Ce sample, the analysis surprisingly led to remarkable differences in composition. Obviously, the homogeneity limit on this side was not reached.

The scanning electron microscopic images of the Au-rich Ce sample, "$CeAu_{2.5}Al_{1.5}$" (Fig. 3), however, revealed three distinct phases, the dark laths of the main phase having a composition near $CeAu_2Al_{1.8}$ (microanalyses of three spots: 1:1.97:1.88, 1:2.00:1.76, and 1:2.04:1.77), grey rounded islands of composition $CeAu_{3.01}Al_{1.37}$ and $CeAu_{3.03}Al_{1.32}$, and a faint grey background of composition $CeAu_{2.71}Al_{0.56}$. The lattice parameters of the $CaBe_2Ge_2$-type phase virtually coincide with those of the stoichiometric phase $CeAu_2Al_2$. The analysis of the two foreign phases in $GdAu_2Al_2$, which were too tiny to be separated, led to an average of $GdAu_{3.23}Al_{1.54}$ and $GdAu_{3.01}Al_{1.46}$, and these values are possibly falsified by contributions from the main phase. It should be kept in mind that for a polyphase material the result of a microanalysis is less reliable than that of a homogeneous material, since there is no guarantee that the electron beam did not interact also with a deeper layer where a different phase may be present. Therefore, we are less intrigued by the deviation from the ideal composition $Ln(Au, Al)_4$, which is also present in the Al-rich samples, and we tentatively conclude that the lower Al limit is close to the ideal 1:2:2 stoichiometry, unless the members of the La···Nd group already possess a slight Al deficit.

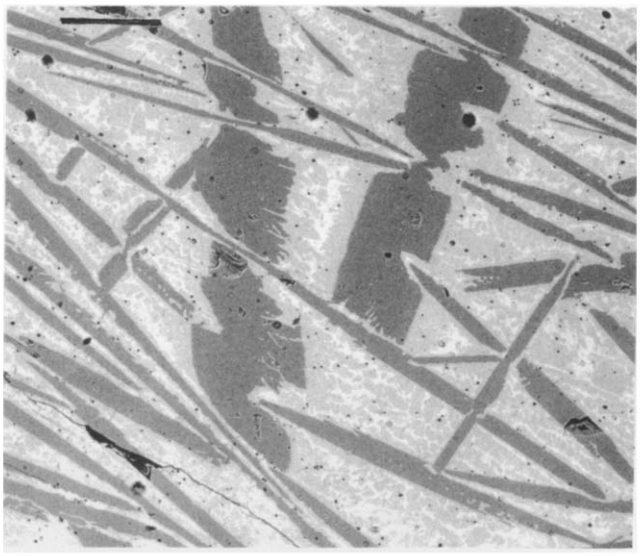

Fig. 3. Back-scattered electron microscope image of the Au-rich sample "$CeAu_{2.5}Al_{1.5}$". The dark lath-shaped areas correspond to the $CaBe_2Ge_2$-type phase. For the grey, rounded areas and for the light background the microanalysis yielded the approximate compositions $CeAu_3Al_{1.34}$ and $CeAu_{2.7}Al_{0.6}$, respectively. Scale bar: 100 μm.

Although the observed *c*-axis discontinuity (or the variable Au/Al ratio) introduces a considerable uncertainty, we tentatively used the *c*-axis to locate the Th and U compounds in the diagram, Fig. 1, in order to derive their effective radii. As expected, the result is only in part satisfactory. The corresponding *c* and *c/a* entries lie in the region of the extrapolation of the right-hand data which we assume to be the correct data for the stoichiometric 1:2:2 members of the series. The differences may reflect the influence of the additional valence electron or, alternatively, point to deviations from the ideal stoichiometry. Nevertheless, the *a*-axis of $ThAu_2Al_2$ closely corresponds to the value which can be predicted from Shannon's [8] Th^{4+} radius (0.94 Å). For six-coordinated U^{3+} and U^{4+} Shannon's radii are 1.165 and 0.89 Å respectively. Judging on the basis of our unit-cell data for UAu_2Al_2 (from which we derive an effective uranium radius $r \approx 0.93$ Å), a uranium valence near 4 (3.85?) may be deduced. Unfortunately, a decision cannot be made on the basis of the magnetic measurements.

If our arguments hold, a compound with an electron deficit should possibly fit into the continuous sequence described here on the basis of the *a*-axis data, and it ought to show a deviation of the *c*-axis in the opposite sense relative to Th^{4+}. For these reasons, the compounds $SrAu_2Al_2$ and $EuAu_2Al_2$ were additionally prepared ($SrAu_2Ga_2$ crystallizes in the same structure type [9]). $SrAu_2Al_2$ has a relatively low melting point, *i.e.* between 700 and 800 °C, and both compounds indeed adopt the $CaBe_2Ge_2$ structure. The lattice parameters, however, do not conform to our expectations: the *a*-axes point to much smaller M^{2+} radii, *i.e.* 1.03 and 1.06 Å for $EuAu_2Al_2$ and $SrAu_2Al_2$, compared to Shannon's values 1.17 and 1.18 Å [8], respectively. However, the *c*-parameters are intermediate between those of the La···Nd group and the off-stoichiometric Sm···Dy group.

Since most of our samples contained at least traces of foreign phases, the magnetic data are not listed here. The impurities, however, did not significantly influence the paramagnetic susceptibility of the 1:2:2 compounds which obeyed the Curie–Weiss law down to fairly low temperatures, with magneton numbers close to the free-ion values. Among all the compounds investigated, a magnetic transition above 2 K, which can be ascribed to the main phase, was detected in only four of them. The Néel temperature of $GdAu_2Al_2$, $TbAu_2Al_2$, and UAu_2Al_2 was found to be near 23, 24, and 15 K, respectively. The Néel temperature of $EuAu_2Al_2$ is probably near 27 K. In our measurements it was masked by a ferromagnetic impurity with a Curie point of 49 K. None of the nonmagnetic compounds revealed a transition to superconductivity above 1.8 K.

Although the exact concentrations of most of our samples are not known with sufficient precision, it can be concluded from the present data that in the system Ln–Au–Al the $CaBe_2Ge_2$ phase occurs with a composition closer to the ideal composition 1:2:2 than in the system Ln–Au–Ga [5]. The homogeneity range extends towards higher Al/Au ratios, however, not up to the composition $LnAuAl_3$, where the structure is bodycentred [10].

Acknowledgments

We thank Mr. Stefan Siegrist for carefully preparing the samples and the Guinier patterns. For the quantitative electron microprobe analyses we are very grateful to Miss Regina Haag and Mr. Urs Bürkli of Sulzer Innotec AG, Winterthur ($LaAu_{1.5}Al_{2.5}$, $CeAu_{1.5}Al_{2.5}$ and $CeAu_{2.5}Al_{1.5}$) and Miss Daniela Sidler, Institute for Crystallography, ETH ($CeAu_2Al_2$, $GdAu_2Al_2$). Dr. Oscar Vogt kindly allowed us to use his moving-sample magnetometer. Last but not least, we are very obliged to Professor H.C. Siegmann as well as to the Swiss National Science Foundation for continuous support.

References

1 F. Hulliger, K. Mattenberger and S. Siegrist, *J. Alloys Comp.*, *190* (1992) 125.
2 F. Hulliger and B. Xue, *J. Alloys Comp.*, *194* (1993) 179.
3 P. Villars and L.D. Calvert, *Pearson's Handbook of Crystallographic Data for Intermetallic Phases*, American Society for Materials, Materials Park, OH, 2nd edn., 1991.
4 T. Takabatake, H. Iwasaki, H. Fujii, S. Ikeda, S. Nishigori, Y. Aoki, T. Suzuki and T. Fujita, *J. Phys. Soc. Jpn.*, *61* (1992) 778.
5 K. Yvon, W. Jeitschko and E. Parthé, *J. Appl. Crystallogr.*, *10* (1977) 73.
6 R. Pöttgen, J.H. Albering, D. Kaczorowski and W. Jeitschko, *J. Alloys Comp.*, *196* (1993) 111.
7 Y.N. Grin, P. Rogl, K. Hiebl, F.E. Wagner and H. Noël, *J. Solid State Chem.*, *70* (1987) 168.
8 R.D. Shannon, *Acta Crystallogr. A*, *32* (1976) 751.
9 G. Cordier and C. Röhr, *Z. Kristallogr.*, *197* (1991) 312.
10 F. Hulliger, to be published.